

Conformal Prediction Regions for Time Series using Linear Complementarity Programming

Matthew Cleaveland[†], Insup Lee[◊], George J. Pappas[†], and Lars Lindemann^{*}

[†] Department of Electrical and Systems Engineering, University of Pennsylvania

[◊] Department of Computer and Information Science, University of Pennsylvania

^{*} Department of Computer Science, University of Southern California

March 2023

Abstract

Conformal prediction is a statistical tool for producing prediction regions of machine learning models that are valid with high probability. However, applying conformal prediction to time series data leads to conservative prediction regions. In fact, to obtain prediction regions over T time steps with confidence $1 - \delta$, previous works require that each individual prediction region is valid with confidence $1 - \delta/T$. We propose an optimization-based method for reducing this conservatism to enable long horizon planning and verification when using learning-enabled time series predictors. Instead of considering prediction errors individually at each time step, we consider a parameterized prediction error over multiple time steps. By optimizing the parameters over an additional dataset, we find prediction regions that are not conservative. We show that this problem can be cast as a mixed integer linear complementarity program (MILCP), which we then relax into a linear complementarity program (LCP). Additionally, we prove that the relaxed LP has the same optimal cost as the original MILCP. Finally, we demonstrate the efficacy of our method on a case study using pedestrian trajectory predictors.

1 Introduction

Autonomous systems perform safety-critical tasks in dynamic and uncertain environments where system errors can be dangerous and costly, e.g., a mistake of a self-driving car navigating in urban traffic. In such scenarios, accurate uncertainty quantification is vital for ensuring safety of learning-enabled systems. In this work, we focus on quantifying uncertainty of time series data. For instance, for a given time series predictor that predicts the future trajectory of a pedestrian, how can we quantify the uncertainty and accuracy of this predictor?

Conformal prediction (CP) has emerged as a popular method for statistical uncertainty quantification [1, 2]. It aims to construct prediction regions that contain the true quantity of interest with a user-defined probability. CP does not require any assumptions about the underlying distribution or the predictor itself. Instead, one only needs calibration data that is exchangeable or independent and identically distributed. That means that CP can seamlessly be applied to learning-enabled

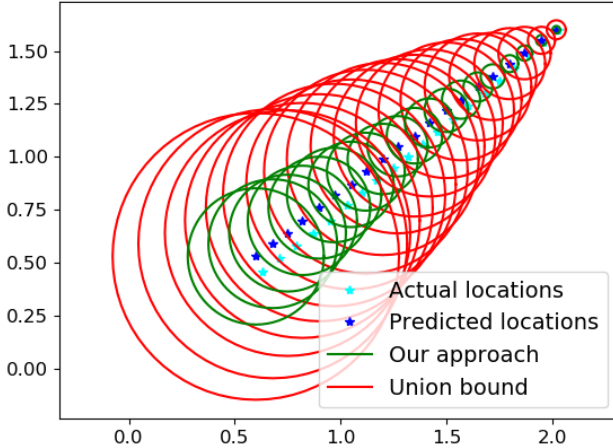


Figure 1: Sample trajectory of a pedestrian (teal stars), the pedestrian predictions using a social LSTM from [6] (blue stars), the conformal prediction regions for our approach (green circles), and the conformal prediction regions for the approach from [7] (red circles). Notably, our approach is less conservative while still providing valid prediction regions.

predictors like neural networks, without the need to analyze the underlying architecture or change the training procedure [3].

One challenge of CP is that its standard variant can not directly be used to construct valid prediction regions for time series. This is because datapoints at different time steps are not exchangeable. Recently, variants of CP have been developed for time series, such as adaptive conformal inference [4, 5]. However, their coverage guarantees are weaker and only asymptotic. While these types of guarantees are useful in many contexts, they are clearly insufficient in many safety-critical applications such as self-driving cars.

In previous works [7–9], this issue was mitigated by instead considering a calibration dataset that consists of full rollouts of the time series, which do not violate the exchangeability assumption. At design time, one runs a separate instance of CP for each of the T time steps of the time series predictor (also referred to as a trajectory predictor). Then at runtime, these CP instances are combined with the predictor’s T predictions to compute prediction regions. However, to obtain prediction regions that are valid over all T time steps with confidence $1 - \delta$, each individual prediction region has to be valid with confidence $1 - \delta/T$.¹ This results in conservative prediction regions.

Contributions: To address this conservatism, this paper proposes constructing prediction regions for time series using linear complementary programming. Our main idea is based on i) mapping trajectory prediction errors to a single parameterized conformal scoring function to avoid union bounding, and ii) finding the optimal parameters from an additional calibration dataset. As opposed to existing works, our method enables non-conservative long horizon planning and verification. Our contributions are as follows:

- We propose the conformal scoring function $R := \max(\alpha_1 R_1, \dots, \alpha_T R_T)$ for time horizon T , prediction errors R_t , and parameters α_t . Using R , we show that we can obtain non-conservative prediction regions with $1 - \delta$ confidence using conformal prediction.

¹A simple union bound or Bonferroni inequality argument can be used to show this result.

- We formulate the problem of finding the parameters α_t that minimize R from an additional calibration dataset as a mixed integer linear complementarity program, and we show how we can derive a linear complementarity program that has the same optimal value.
- On a pedestrian case study, we demonstrate that our method produces much smaller valid conformal prediction regions compared to [7–9], see Figure 1.

1.1 Related Work

Conformal prediction was originally proposed by Vovk in [1, 2] to quantify uncertainty of prediction models. The original method, however, required training a prediction model for each calibration datapoint, which is computationally intractable for learning-enabled predictors. Inductive conformal prediction, also referred to as split conformal prediction, addresses this issue by splitting the calibration data into two sets, one used for training the prediction model and one for applying conformal prediction [10]. Split conformal prediction has been extended to provide conditional probabilistic guarantees [11], to handle distribution shifts [12, 13], and to allow for quantile regression [14]. Further, split conformal prediction has been used to construct probably approximately correct prediction sets for machine learning models [15, 16], to perform out-of-distribution detection [17, 18], to guarantee safety in autonomous systems [19], and to quantify uncertainty for F1/10 car motion predictions [20]. Additionally, in [21] the authors encode the width of the generated prediction sets directly into the loss function of a neural network during training.

However, the aforementioned methods cannot directly be applied to time series data. Multiple works have adapted conformal prediction algorithms for the time series domain, including enbpi [22], adaptive conformal inference [4], and fully adaptive conformal inference [23, 24]. However, they only provide averaged coverage guarantees over long horizons. Regardless, these methods have been used for analyzing financial market data [25], synthesizing safe robot controllers [26], and dynamically allocating compute resources [27]. For a more comprehensive overview of the conformal prediction landscape see [3].

Our paper is motivated by [7–9]. These works apply inductive conformal prediction in a time series setting, which requires construction individual prediction regions with confidence $1 - \delta/T$ to obtain $1 - \delta$ coverage for all time steps. This results in unnecessarily conservative prediction regions that are impractical for downstream tasks such as motion planning. We overcome this limitation by considering a parameterized conformal scoring function that is defined over multiple time steps.

2 Background

In this section, we present background on time series predictors and split conformal prediction for time series.

2.1 Time Series Predictors

We want to predict future values Y_1, \dots, Y_T of a time series for a prediction horizon of T from past observed values $Y_{T_{obs}}, \dots, Y_0$ for an observation length of T_{obs} . Let \mathcal{D} denote an unknown distribution over a finite-horizon time series $Y := (Y_{T_{obs}}, \dots, Y_0, Y_1, \dots, Y_T)$, i.e., let

$$(Y_{T_{obs}}, \dots, Y_0, Y_1, \dots, Y_T) \sim \mathcal{D}$$

denote a random trajectory drawn from \mathcal{D} where $Y_t \in \mathbb{R}^m$ is the value at time t . We make no assumptions about the distribution \mathcal{D} , but we do assume availability of a calibration dataset in which each trajectory is drawn independently from \mathcal{D} . Particularly, define

$$D_{cal} := \{Y^{(1)}, \dots, Y^{(n)}\}$$

where the element $Y^{(i)} := (Y_{T_{obs}}^{(i)}, \dots, Y_0^{(i)}, Y_1^{(i)}, \dots, Y_T^{(i)})$ is independently drawn from \mathcal{D} , i.e., $Y^{(i)} \sim \mathcal{D}$.

A key challenge lies in constructing accurate predictions of future values Y_1, \dots, Y_T of the time series. We assume here that we are already given a time series predictor $h : \mathbb{R}^{m(T_{obs}+1)} \rightarrow \mathbb{R}^{mT}$ that maps $(Y_{T_{obs}}, \dots, Y_0)$ to estimates of the next T values (Y_1, \dots, Y_T) , denoted as

$$(\hat{Y}_1, \dots, \hat{Y}_T) := h(Y_{T_{obs}}, \dots, Y_0).$$

We make no assumptions about h . For example, it can be a long short-term memory network (LSTM) [28] or a sliding linear predictor with extended Kalman filters [29]. Using the predictor h , we can obtain prediction for the calibration data in D_{cal} . Specifically, for each $Y^{(i)} \in D_{cal}$, we obtain

$$(\hat{Y}_1^{(i)}, \dots, \hat{Y}_T^{(i)}) := h(Y_{T_{obs}}^{(i)}, \dots, Y_0^{(i)}). \quad (1)$$

The predictor h may not be exact, and the inaccuracy of its predictions $(\hat{Y}_1, \dots, \hat{Y}_T)$ is unknown. We will quantify prediction uncertainty using the calibration dataset D_{cal} and split conformal prediction, which we introduce next.

2.2 Split Conformal Prediction

Conformal prediction was introduced in [1, 2] to obtain valid prediction regions for complex predictive models such as neural networks without making assumptions on the distribution of the underlying data. Split conformal prediction is a computationally tractable variant of conformal prediction [10] where it is assumed that a calibration dataset is available that has not been used to train the predictor. Let $R^{(0)}, \dots, R^{(k)}$ be $k+1$ exchangeable random variables.² The variable $R^{(i)}$ is usually referred to as the *nonconformity score*. In supervised learning, it is often defined as $R^{(i)} := \|Z^{(i)} - \mu(X^{(i)})\|$ where the predictor μ attempts to predict the output $Z^{(i)}$ based on the input $X^{(i)}$. A large nonconformity score indicates a poor predictive model. Our goal is to obtain a prediction region for $R^{(0)}$ based on $R^{(1)}, \dots, R^{(k)}$, i.e., the random variable $R^{(0)}$ should be contained within the prediction region with high probability.

Formally, given a failure probability $\bar{\delta} \in (0, 1)$, we want to construct a valid prediction region C so that³

$$\text{Prob}(R^{(0)} \leq C) \geq 1 - \bar{\delta}. \quad (2)$$

²Formally, this means that the joint distribution of $R^{(0)}, \dots, R^{(k)}$ is the same as the joint distribution of $R^{(\sigma(0))}, \dots, R^{(\sigma(k))}$ for any permutation σ on $\{0, \dots, k\}$. Intuitively, exchangeability is a slightly weaker form of independent and identically distributed (i.i.d.) random variables.

³More formally, we would have to write $C(R^{(1)}, \dots, R^{(k)})$ as the prediction region C is a function of $R^{(1)}, \dots, R^{(k)}$. For this reason, the probability measure P is defined over the product measure of $R^{(0)}, \dots, R^{(k)}$.

We pick $C := \text{Quantile}(\{R^{(1)}, \dots, R^{(n_1)}, \infty\}, 1 - \bar{\delta})$ which is the $(1 - \bar{\delta})$ th quantile of the empirical distribution of the values $R^{(1)}, \dots, R^{(k)}$ and ∞ . Alternatively, by assuming that $R^{(1)}, \dots, R^{(k)}$ are sorted in non-decreasing order and by adding $R^{(k+1)} := \infty$, we can equivalently obtain $C := R^{(p)}$ where $p := \lceil (k+1)(1 - \bar{\delta}) \rceil$ with $\lceil \cdot \rceil$ being the ceiling function, i.e., C is the p th smallest nonconformity score. By a quantile argument, see [12, Lemma 1], one can prove that this choice of C satisfies Equation (2). We remark that $k \geq \lceil (k+1)(1 - \bar{\delta}) \rceil$ is required to hold to obtain meaningful, i.e., bounded, prediction regions.

Remark 1. Note that split conformal prediction assumes that the non-conformity scores $R^{(0)}, \dots, R^{(k)}$ are exchangeable. This complicates its use for time series data where Y_{t+1} generally depends on Y_t . However, with a calibration dataset D_{cal} of trajectories independently drawn from \mathcal{D} , the application of conformal prediction is possible [7–9]. In summary, one defines T non-conformity scores $R_t^{(i)} := \|\hat{Y}_t^{(i)} - Y_t^{(i)}\|$ for each time $t \in \{1, \dots, T\}$ and each calibration trajectory $Y^{(i)} \in D_{\text{cal}}$; $R_t^{(i)}$ can be interpreted as the t -step ahead prediction error. Using conformal prediction, for each time t we can then construct a prediction region C_t so that $\text{Prob}(\|\hat{Y}_t - Y_t\| \leq C_t) \geq 1 - \bar{\delta}$. To then obtain a prediction region over all time steps, i.e., $\text{Prob}(\|\hat{Y}_t - Y_t\| \leq C_t, \forall t \in \{1, \dots, T\}) \geq 1 - \delta$, we simply set $\bar{\delta} := \delta/T$. As previously mentioned, this results in conservative prediction regions that are not practical.

3 Problem Formulation and Main Idea

Our goal is to construct valid conformal prediction regions for time series. The main idea is to use a parameterized non-conformity score that considers predictions errors over all T time steps. Particularly, in this paper we consider the non-conformity score

$$R := \max(\alpha_1 R_p(Y_1, \hat{Y}_1), \dots, \alpha_T R_p(Y_T, \hat{Y}_T)) \quad (3)$$

where $\alpha_1, \dots, \alpha_T > 0$ are parameters and where R_p is the prediction error for an individual time step. For the purpose of this paper, we use the Euclidean distance between the actual and the predicted value of the time series at time t as

$$R_p(Y_t, \hat{Y}_t) := \|Y_t - \hat{Y}_t\| \quad (4)$$

We note that R_p can in general be any function of Y_t and \hat{Y}_t . Within the context of this paper, however, we set R_p to be the Euclidean distance between Y_t and \hat{Y}_t as in (4).

Taking the maximum prediction error over all T time steps as in equation (4) will allow us to avoid the overly conservative prediction regions from [7–9] as we, in our proof, do not need to union bound over the individual prediction errors. However, the choice of the parameters $\alpha_1, \dots, \alpha_T$ is now important. If we apply conformal prediction as described in Section 2.2 to the nonconformity score in (3) with $\alpha_1 = \dots = \alpha_T = 1$, this would typically result in obtaining large prediction regions for the first time step since usually prediction errors get larger with increasing time, i.e., $R_p(Y_T, \hat{Y}_T)$ in (3) would dominate so that $R = R_p(Y_T, \hat{Y}_T)$. Introducing the parameters $\alpha_1, \dots, \alpha_T$ allows for weighting the different time steps, and we generally expect α_t for larger times to be smaller than α_t for smaller times.

Given the parameterized function R as in Equation (3) and a failure threshold of $\delta \in (0, 1)$, we are in this paper particularly interested in computing the parameters $\alpha_1, \dots, \alpha_T$ that minimize the

constant C that satisfies

$$\text{Prob}(R \leq C) \geq 1 - \delta.$$

For given parameters $\alpha_1, \dots, \alpha_T$, note that the constant C can be found by applying conformal prediction to the nonconformity score R using the calibration set D_{cal} . When we have found this constant C , we know that

$$\text{Prob}(\|Y_t - \hat{Y}_t\| \leq C/\alpha_t, \forall t \in \{1, \dots, T\}) \geq 1 - \delta.$$

To solve the aforementioned problem, we split the calibration dataset D_{cal} into two sets $D_{cal,1}$ and $D_{cal,2}$. We will use the first calibration dataset $D_{cal,1}$ to compute the values of $\alpha_1, \dots, \alpha_T$ that give the smallest prediction region C for R (see Section 4). In a next step, we use these parameters that now fully define the nonconformity score R along with the second calibration dataset $D_{cal,2}$ to construct valid prediction regions via conformal prediction (see Section 5).

4 Nonconformity Scores for Time-Series via Linear Programming

We first have to set up some notation. Let us denote the elements of the first calibration dataset as $D_{cal,1} := \{Y^{(1)}, \dots, Y^{(n_1)}\}$ where $n_1 > 0$ is the size of the first calibration dataset. Recall that each element $Y^{(i)}$ of $D_{cal,1}$ is defined as $Y^{(i)} = (Y_{T_{obs}}^{(i)}, \dots, Y_0^{(i)}, Y_1^{(i)}, \dots, Y_T^{(i)})$. Using the trajectory predictor h , we obtain predictions $(\hat{Y}_1^{(i)}, \dots, \hat{Y}_T^{(i)})$ for $(Y_1^{(i)}, \dots, Y_T^{(i)})$ as per equation (1).

We then compute the prediction error $R_t^{(i)}$ according to equation (4) for each calibration trajectory and for each time step, i.e., for each $t \in \{1, \dots, T\}$ and $i \in \{1, \dots, n_1\}$. More formally, we compute for each calibration trajectory

$$R_t^{(i)} := R_p(Y_t^{(i)}, \hat{Y}_t^{(i)}). \quad (5)$$

We can now cast the problem of finding the parameters $\alpha_1, \dots, \alpha_T$ as the following optimization problem.

$$\min_{\alpha_1, \dots, \alpha_T} \text{Quantile}(\{R^{(1)}, \dots, R^{(n_1)}, \infty\}, 1 - \delta) \quad (6a)$$

$$\text{s.t. } R^{(i)} = \max(\alpha_1 R_1^{(i)}, \dots, \alpha_T R_T^{(i)}), i = 1, \dots, n_1 \quad (6b)$$

$$\sum_{j=1}^T \alpha_j = 1 \quad (6c)$$

$$\alpha_j > 0, j = 1, \dots, T \quad (6d)$$

where we recall that $\text{Quantile}(\{R^{(1)}, \dots, R^{(n_1)}, \infty\}, 1 - \delta)$ denotes the empirical $1 - \delta$ quantile of the set $\{R^{(1)}, \dots, R^{(n_1)}, \infty\}$. Equations (6c) and (6d) normalize $\alpha_1, \dots, \alpha_T$ and ensure them to be positive.

Remark 2. *We note that the optimization problem in equation (6) is always feasible. This follows since any set of parameters $\alpha_1, \dots, \alpha_T$ that satisfy Equations (6c) and (6d) constitute a feasible solution to (6).*

To solve the optimization problem in equation (6), we transform it into a linear complementarity program [30] that has the same optimal value as (6). To do so, we first reformulate the $\max()$ operator in equation (6b) as a set of mixed integer linear program (MILP) constraints, which we then transform into a set of linear program constraints. We show that this transformation preserves the optimal value of (6) (see Section 4.1). Then, we reformulate the Quantile function from equation (6a) into a linear program (LP) that we further reformulate using its KKT conditions (see Section 4.2), resulting in a linear complementarity program.

4.1 Reformulating the Max Operator

We first use ideas from [31, 32] for encoding the max operator in (6b) as an MILP. Therefore, we introduce the binary variables $b_t^{(i)} \in \{0, 1\}$ for each time $t \in \{1, \dots, T\}$ and calibration trajectory $i \in \{1, \dots, n_1\}$. The equality constraint $R^{(i)} = \max(\alpha_1 R_1^{(i)}, \dots, \alpha_T R_T^{(i)})$ in equation (6b) is then equivalent to the following MILP constraints:

$$R^{(i)} \geq \alpha_t R_t^{(i)}, \quad t = 1, \dots, T \quad (7a)$$

$$R^{(i)} \leq \alpha_t R_t^{(i)} + (1 - b_t^{(i)})M, \quad t = 1, \dots, T \quad (7b)$$

$$\sum_{t=1}^T b_t^{(i)} = 1 \quad (7c)$$

$$b_t^{(i)} \in \{0, 1\}, \quad t = 1, \dots, T \quad (7d)$$

where $M > 0$ is a sufficiently large and positive constant.⁴

By replacing the max operator in Equation (6b) with the MILP encoding in Equation (7), we arrive at the following optimization problem:

$$\min_{\alpha_1, \dots, \alpha_T} \text{Quantile}(\{R^{(1)}, \dots, R^{(n_1)}, \infty\}, 1 - \delta) \quad (8a)$$

$$\text{s.t.} \quad R^{(i)} \geq \alpha_t R_t^{(i)}, \quad i = 1, \dots, n_1 \wedge t = 1, \dots, T \quad (8b)$$

$$R^{(i)} \leq \alpha_t R_t^{(i)} + (1 - b_t^{(i)})M, \quad i = 1, \dots, n_1 \wedge t = 1, \dots, T \quad (8c)$$

$$\sum_{t=1}^T b_t^{(i)} = 1 \quad (8d)$$

$$b_t^{(i)} \in \{0, 1\}, \quad t = 1, \dots, T \quad (8e)$$

$$(6c), (6d)$$

The constraints in (8) are linear in their parameters, i.e., in α_t , $R^{(i)}$, and $b_t^{(i)}$. The cost function in (8a) can be reformulated as a linear complementarity program (LCP), as shown in the next section. Thus, (8) is an MILCP since the $b_t^{(i)}$ variables are binary due to equation (8e). Commercial solvers can solve MILCPs, but they present scalability issues for larger time horizons T and calibration data n_1 . Therefore, we present an LCP reformulation of (8) which will achieve the same optimality in terms of the constraint function (8a) while providing better scalability.

⁴See [31] for the exact conditions required of M .

4.1.1 Linear complementarity relaxation of the MILCP in (8)

We start by removing the upper bound on $R^{(i)}$ in equation (8c) and the binary variables $b_t^{(i)}$ in equations (8d) and (8e) from the MILCP in (8). This results in the optimization problem:

$$\min_{\alpha_1, \dots, \alpha_T} \text{Quantile}(\{R^{(1)}, \dots, R^{(n_1)}, \infty\}, 1 - \delta) \quad (9a)$$

$$\text{s.t. } R^{(i)} \geq \alpha_t R_t^{(i)}, \quad i = 1, \dots, n_1 \wedge t = 1, \dots, T \quad (9b)$$

(6c), (6d)

Note that the above optimization problem is now a linear complementarity program due to the removal of the binary variables $b_t^{(i)}$. While the LCP in (9) is clearly computationally more tractable than the MILCP in (8), one may ask in what way the optimal solutions of these two optimization problems are related. We next prove that the optimal values (in terms of the cost functions in (8a) and (9a)) of the two optimization problems (8) and (9) are the same.

Theorem 1. *Let $\delta \in (0, 1)$ be a failure rate and $R_t^{(i)}$ be the prediction errors as in (5) for times $t \in \{1, \dots, T\}$ and calibration trajectories $i \in \{1, \dots, n_1\}$ from $D_{\text{cal},1}$. Then, the optimal cost values of the optimization problems (8) and (9) are equivalent.*

Proof. Assume that $\alpha_1^*, \dots, \alpha_T^*, R^{(1),*}, \dots, R^{(n_1),*}$ is an optimal solution to the optimization problem in equation (9). We will first show that we can use $\alpha_1^*, \dots, \alpha_T^*, R^{(1),*}, \dots, R^{(n_1),*}$ to construct a feasible solution to the optimization problem in (8), which we denote by $\bar{\alpha}_1^*, \dots, \bar{\alpha}_T^*, \bar{R}^{(1),*}, \dots, \bar{R}^{(n_1),*}$, without altering the optimal value of the objective function. Particularly, let

$$\bar{\alpha}_t^* := \alpha_t^*, \quad t = 1, \dots, T \quad (10a)$$

$$\bar{R}^{(i),*} := \max(\bar{\alpha}_1^* R_1^{(i)}, \dots, \bar{\alpha}_T^* R_T^{(i)}), \quad i = 1, \dots, n_1 \quad (10b)$$

Note that there exists binary variables $\bar{b}_t^{(i)}$ along with which $\bar{\alpha}_1^*, \dots, \bar{\alpha}_T^*, \bar{R}^{(1),*}, \dots, \bar{R}^{(n_1),*}$ are a feasible solution to the optimization problem in (8). This follows since (10a) satisfies (6c) and (6d) and (10b) satisfies (6b) and consequently (8b-8d) for appropriate choices of $\bar{b}_t^{(i)}$ (and M).

Note specifically that $\bar{\alpha}_t^*$ and α_t^* are the same, while this does not necessarily hold for $R^{(i),*}$ and $\bar{R}^{(i),*}$. However, it is guaranteed that $\bar{R}^{(i),*} \leq R^{(i),*} \forall i = 1, \dots, n_1$ as the constraint in (9b) ensures that $R^{(i),*}$ is lower bounded by $\max(\alpha_1^* R_1^{(i)}, \dots, \alpha_T^* R_T^{(i)}) = \max(\bar{\alpha}_1^* R_1^{(i)}, \dots, \bar{\alpha}_T^* R_T^{(i)})$. Since the Quantile function is a monotone operator (its value is non-increasing if inputs are non-increasing), the value of the objective function in (8) that corresponds to $\bar{\alpha}_1^*, \dots, \bar{\alpha}_T^*, \dots, \bar{R}^{(1),*}, \bar{R}^{(n_1),*}$ can not be greater than the value of the objective function in (9) that corresponds to $\alpha_1^*, \dots, \alpha_T^*, R^{(1),*}, \dots, R^{(n_1),*}$.

At the same time, we note that the optimal value of the optimization problem in (9) cannot be greater than the optimal value of the optimization problem in (8) because it has strictly fewer constraints than (9) so that the feasible set of (9) contains the feasible of (8). As a consequence, the optimal values of (8) and (9) are equivalent. \square

Note that Theorem 1 guarantees that the optimal values of the optimization problems in (8) and (9) are equivalent. However, we do not guarantee that the optimal parameters $\alpha_1^*, \dots, \alpha_T^*$ obtained by solving (8) and (9) will be the same as the optimization problem in (8) may have multiple optimal solutions $\alpha_1^*, \dots, \alpha_T^*$. Nonetheless, the linear reformulation in (9) is computationally tractable and cost optimal. In our experiments in Section 6.3.1, we also show that we obtain parameters from (8) and (9) that are almost equivalent.

4.2 Reformulating the Quantile Function

We note that the Quantile function in (6a) can be written as the following linear program [33]:

$$\begin{aligned} & \text{Quantile}(\{R^{(1)}, \dots, R^{(n_1)}\}, 1 - \delta) \\ &= \underset{q}{\text{argmin}} \sum_{i=1}^{n_1} ((1 - \delta)e_i^+ + \delta e_i^-) \end{aligned} \quad (11a)$$

$$\text{s.t. } e_i^+ - e_i^- = R^{(i)} - q, \quad i = 1, \dots, n_1 \quad (11b)$$

$$e_i^+, e_i^- \geq 0, \quad i = 1, \dots, n_1 \quad (11c)$$

where the optimal solution q of (11) is equivalent to $\text{Quantile}(\{R^{(1)}, \dots, R^{(n_1)}\}, 1 - \delta)$. However, we note that we can not directly replace $\text{Quantile}(\{R^{(1)}, \dots, R^{(n_1)}\}, 1 - \delta)$ in the optimization problem in (6a) with the linear program from equation (11) as that would result in a problem with an objective function that is itself an optimization problem. To address this issue, we replace the optimization problem in (11) with its KKT conditions that are as follows:

$$(1 - \delta) - u_i^+ + v_i = 0, \quad i = 1, \dots, n_1 \quad (12a)$$

$$\delta - u_i^- - v_i = 0, \quad i = 1, \dots, n_1 \quad (12b)$$

$$\sum_{i=1}^{n_1} v_i = 0 \quad (12c)$$

$$u_i^+ e_i^+ = 0, \quad i = 1, \dots, n_1 \quad (12d)$$

$$u_i^- e_i^- = 0, \quad i = 1, \dots, n_1 \quad (12e)$$

$$e_i^+ \geq 0, \quad i = 1, \dots, n_1 \quad (12f)$$

$$e_i^- \geq 0, \quad i = 1, \dots, n_1 \quad (12g)$$

$$e_i^+ + q - e_i^- - R^{(i)} = 0, \quad i = 1, \dots, n_1 \quad (12h)$$

$$u_i^+ \geq 0, \quad i = 1, \dots, n_1 \quad (12i)$$

$$u_i^- \geq 0, \quad i = 1, \dots, n_1 \quad (12j)$$

Here, the constraints (12a), (12b) and (12c) encode the stationarity condition, the constraints (12d) and (12e) encode complementary slackness, the constraints (12f), (12g), and (12h) encode primal feasibility, and the constraints (12i) and (12j) encode dual feasibility. This is an LCP because every constraint is either linear (((12a)-(12c)) and ((12f)-(12j))) or an equality constraint stating the multiple of two positive variables equals 0 ((12d) and (12e)).⁵ Despite the slight non-linearity, LCPs can be efficiently solved with existing tools [34].

Because feasible linear optimization problems have zero duality gap [35], any solution to the KKT conditions in (12) is also an optimal solution to Problem (11).

4.3 Summarizing the Optimization Programs

Based on the results from the previous subsections, we can formulate two optimization problems that solve (6).

⁵These constraints ensure that one of the two variables equals 0.

First, we can exactly solve (6) by replacing the max operator in (6b) with the MILP in (7) and the quantile function in (6a) with its KKT conditions in (12). The following result follows by construction (for sufficiently large M).

Proposition 1. *The mixed integer linear complementarity program*

$$\begin{aligned} & \min_{q, \alpha_1, \dots, \alpha_T} q & (13a) \\ & \text{s.t.} \quad (8b), (8c), (8d), (8e) \\ & \quad (12a), (12b), (12c), (12d), (12e) \\ & \quad (12f), (12g), (12h), (12i), (12j) \\ & \quad (6c), (6d) \end{aligned}$$

is equivalent to the optimization problem in (6).

Second, by further removing the upper bound from the max operator as described in Section 4.1.1, we can solve a linear complementarity program that has the same optimal cost value as (6). This result follows from Theorem 2.

Proposition 2. *The linear complementarity program*

$$\begin{aligned} & \min_{q, \alpha_1, \dots, \alpha_T} q & (14a) \\ & \text{s.t.} \quad (8b) \\ & \quad (12a), (12b), (12c), (12d), (12e) \\ & \quad (12f), (12g), (12h), (12i), (12j) \\ & \quad (6c), (6d) \end{aligned}$$

has the same optimal value as the optimization problem (6).

5 Conformal Prediction Regions for Time-Series

Finally, after obtaining the parameters $\alpha_1, \dots, \alpha_T$ from the first calibration dataset $D_{cal,1}$ by solving (13) or (14), we can apply conformal prediction with the non-conformity score R as defined in (3) to obtain prediction regions for time series. We do so by following Section 2.2 and using the second calibration dataset $D_{cal,2}$.

More formally, let us denote the elements of the second calibration dataset as $D_{cal,2} := \{Y^{(n_1+1)}, \dots, Y^{(n)}\}$ where $n - n_1 > 0$ is the size of the second calibration dataset.⁶ For each calibration trajectory $i \in \{n_1 + 1, \dots, n\}$, we compute the nonconformity score as

$$R^{(i)} := \max \left(\alpha_1 R_p(Y_1^{(i)}, \hat{Y}_1^{(i)}), \dots, \alpha_T R_p(Y_T^{(i)}, \hat{Y}_T^{(i)}) \right). \quad (15)$$

We are now ready to state the final result of our paper in which we obtain prediction regions for $R := \max(\alpha_1 R_p(y_1, \hat{y}_1), \dots, \alpha_T R_p(y_T, \hat{y}_T))$.

⁶Recall the n is the size of D_{cal} and n_1 is the size of $D_{cal,1}$.

Theorem 2. Let Y be a trajectory drawn from \mathcal{D} and let $\hat{Y} = h(Y_{T_{obs}}, \dots, Y_0)$ be predictions from the time series predictor h . Let $\delta \in (0, 1)$ be a failure rate and $R_t^{(i)}$ be the prediction error as in (5) for times $t \in \{1, \dots, T\}$ and calibration trajectories $i \in \{1, \dots, n_1\}$ from $D_{cal,1}$. Let $\alpha_1, \dots, \alpha_T$ be obtained by solving (13) or (14). Further, let $R^{(i)}$ be the nonconformity score as in (15) for calibration trajectories $i \in \{n_1+1, \dots, n\}$ from $D_{cal,2}$. Finally, let $R = \max(\alpha_1 R_p(Y_1, \hat{Y}_1), \dots, \alpha_T R_p(Y_T, \hat{Y}_T))$. It then holds that

$$\text{Prob}(R \leq C) \geq 1 - \delta \quad (16)$$

where $C := \text{Quantile}(\{R^{(n_1+1)}, \dots, R^{(n)}\}, 1 - \delta)$.

Proof. Since $\alpha_1, \dots, \alpha_T$ are obtained from $D_{cal,1}$, the non-conformity scores $R^{(i)}$ which are computed from $D_{cal,2}$ are exchangeable. Consequently, we can apply [12, Lemma 1] to get that Equation (16) holds. \square

We point out the necessity to split the dataset D_{cal} into the datasets $D_{cal,1}$ and $D_{cal,2}$ to conform to the exchangeability assumption in conformal prediction. To convert equation (16) into practical conformal prediction regions, note that

$$\begin{aligned} R &= \max(\alpha_1 \|Y_1 - \hat{Y}_1\|, \dots, \alpha_T \|Y_T - \hat{Y}_T\|) \leq C \\ \Leftrightarrow \quad & \|Y_t - \hat{Y}_t\| \leq C/\alpha_t \quad \forall t \in \{1, \dots, T\} \end{aligned}$$

Intuitively, the conformal prediction regions provide geometric balls of radius C/α_t around each prediction \hat{y}_t due to the use of the Euclidean norm. For an example, we refer to Figure 1. We remark that other choices of the prediction R_p may lead to different shapes. We summarize this result next.

Corollary 1. Let all conditions of Theorem 2 hold. Then, it follows that

$$\text{Prob}(\|Y_t - \hat{Y}_t\| \leq C/\alpha_t \quad \forall t \in \{1, \dots, T\}) \geq 1 - \delta.$$

6 Case Study

We compare our method to the approach from [7–9] that is described in Section 2.2, which requires conservative union bounding to obtain valid prediction regions. We colloquially refer to this method as the union bound approach. We use Gurobi [36] to solve the optimization problems on a Windows machine running an Intel i7-8550U CPU with 4 cores and 16GB of RAM. The code for this case study can be found on Github.

6.1 ORCA and LSTM

For the case study, we analyze pedestrian location predictions using data generated from the ORCA simulator [37]. We use the social LSTM [6] architecture to make predictions up to 2.5 seconds into the future at a rate of 8Hz (so that $T = 20$ predictions in total) with the previous 2.5 seconds as input (so that $T_{obs} = 20$) using the trajnet++ framework [38]. For the exact details of training, we refer the reader to our previous work in [7].

We collect a dataset of 1291 trajectories, each with 20 future predictions. We randomly select 646 of these points for D_{cal} and use the rest to form D_{val} , which we use for validation. We randomly select 50 trajectories from D_{cal} for $D_{cal,1}$ (to compute the α values) and the remaining trajectories for $D_{cal,2}$ (to compute the conformal prediction regions). We use (14) to compute the α values. Throughout this section, we set $\delta := 0.05$. In Section 6.2 we show the results for one realization of this process and in Section 6.3 we run 100 trials to statistically analyze the results⁷

6.2 Single Trial Analysis

For one of the realizations, the α values are shown in Table 1. They decrease as the prediction horizon increases, which is what we expect as the prediction error generally increases over time. For that same trial, a trajectory of the actual and predicted pedestrian locations is shown alongside the conformal prediction regions in Figure 1. Figure 2 shows scatter plots of the prediction errors over D_{val} and the conformal prediction region radii for 3 time steps.

Table 1: Values of α parameters for ORCA case study.

Time step	α	Time step	α
1	0.21134	11	0.0267
2	0.1495	12	0.0229
3	0.1057	13	0.0207
4	0.0945	14	0.0189
5	0.0668	15	0.0171
6	0.0555	16	0.0158
7	0.0423	17	0.0148
8	0.0371	18	0.0138
9	0.0330	19	0.0125
10	0.0290	20	0.0118

6.3 Statistical Analysis

Over 100 trials, the average (trajectory level) coverage for our approach was 0.9558 and the average coverage for the union bound approach was 0.9945. Histograms of the validation coverage for the two approaches are shown in Figure 3. The union bound approach has larger coverage due to the conservatism introduced by union bounding. However, this highlights that our method produces valid conformal prediction regions that are not overly conservative and significantly tighter than previous approaches.

To further quantify the how much less conservative our prediction regions are, we also computed the average size of the conformal regions for each time horizon, which are shown in Figure 4. This again demonstrates that our approach results in significantly smaller prediction regions.

⁷This is a random process, as splitting the data into $D_{cal,1}$, $D_{cal,2}$, and D_{val} is random and the guarantees of conformal prediction are taken over the distribution of the calibration and validation data. Thus we need to statistically analyze the results.

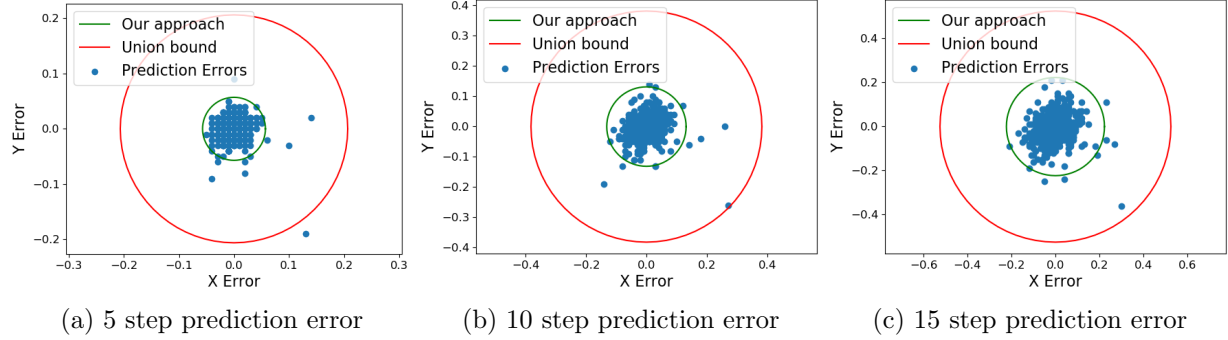


Figure 2: Conformal prediction regions and errors for various prediction horizons. The green circles show the regions produced by our approach and the red circles show the regions produced by the union bound approach. Notably, our approach produces much tighter valid predictions regions.

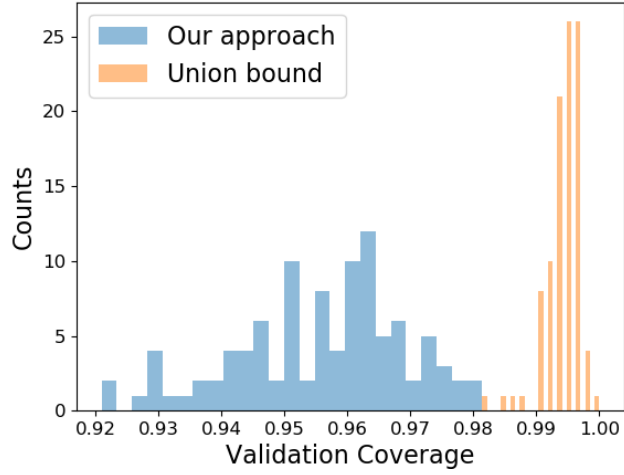


Figure 3: Validation coverage histograms for each of the two methods for 100 trials.

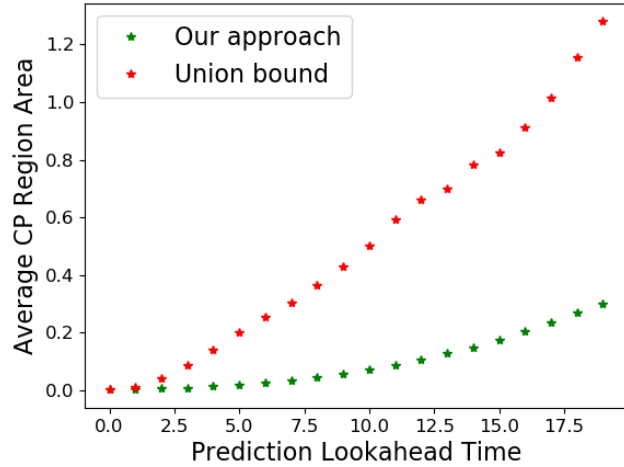


Figure 4: Average area of the conformal prediction regions for each of the three approaches over 100 trials.

6.3.1 Original v. Relaxed Problem Difference

For each trial we also computed the objective function and α values using Equation (13) to compare to those computed using Equation (14). The average difference between the objective function values is $1.847 * 10^{-9}$. The average l^2 norm difference between the α values is $3.495 * 10^{-7}$ and the largest l^2 norm difference is $3.453 * 10^{-5}$. These differences are well within the solver’s default tolerance of 10^{-4} , which empirically validates the equivalence from Theorem 1. The average runtime for solving the original problem was 0.525 seconds and the relaxed problem was 0.207 seconds. So the relaxation cuts the computation time in half.

7 Conclusion

In this paper, we have presented a method for producing conformal prediction regions for time series data that are significantly tighter than previous approaches. To do this, we define a parameterized non-conformity score function and use optimization to fit the function to calibration data. This allows us to use standard inductive conformal prediction to get valid prediction regions. For future work, we plan to integrate our conformal prediction approach into planning and control frameworks and apply parameterized non-conformity score functions to the non-time series setting.

Acknowledgements

This work was generously supported by NSF award CPS-2038873.

References

- [1] G. Shafer and V. Vovk, “A tutorial on conformal prediction.” *Journal of Machine Learning Research*, vol. 9, no. 3, 2008.
- [2] V. Vovk, A. Gammerman, and G. Shafer, *Algorithmic learning in a random world*. Springer Science & Business Media, 2005.
- [3] A. N. Angelopoulos and S. Bates, “A gentle introduction to conformal prediction and distribution-free uncertainty quantification,” *arXiv preprint arXiv:2107.07511*, 2021.
- [4] I. Gibbs and E. Candes, “Adaptive conformal inference under distribution shift,” *Advances in Neural Information Processing Systems*, vol. 34, pp. 1660–1672, 2021.
- [5] M. Zaffran, O. Féron, Y. Goude, J. Josse, and A. Dieuleveut, “Adaptive conformal predictions for time series,” in *International Conference on Machine Learning*. PMLR, 2022, pp. 25 834–25 866.
- [6] A. Alahi, K. Goel, V. Ramanathan, A. Robicquet, L. Fei-Fei, and S. Savarese, “Social lstm: Human trajectory prediction in crowded spaces,” in *Proceedings of the IEEE conference on computer vision and pattern recognition*, 2016, pp. 961–971.
- [7] L. Lindemann, M. Cleaveland, G. Shim, and G. J. Pappas, “Safe planning in dynamic environments using conformal prediction,” *arXiv preprint arXiv:2210.10254*, 2022.

[8] K. Stankeviciute, A. M Alaa, and M. van der Schaar, “Conformal time-series forecasting,” *Advances in Neural Information Processing Systems*, vol. 34, pp. 6216–6228, 2021.

[9] L. Lindemann, X. Qin, J. V. Deshmukh, and G. J. Pappas, “Conformal prediction for stl runtime verification,” *arXiv preprint arXiv:2211.01539*, 2022.

[10] H. Papadopoulos, “Inductive conformal prediction: Theory and application to neural networks,” in *Tools in artificial intelligence*. Citeseer, 2008.

[11] V. Vovk, “Conditional validity of inductive conformal predictors,” in *Asian conference on machine learning*. PMLR, 2012, pp. 475–490.

[12] R. J. Tibshirani, R. Foygel Barber, E. Candes, and A. Ramdas, “Conformal prediction under covariate shift,” *Advances in neural information processing systems*, vol. 32, 2019.

[13] C. Fannjiang, S. Bates, A. Angelopoulos, J. Listgarten, and M. I. Jordan, “Conformal prediction for the design problem,” *arXiv preprint arXiv:2202.03613*, 2022.

[14] Y. Romano, E. Patterson, and E. Candes, “Conformalized quantile regression,” *Advances in neural information processing systems*, vol. 32, 2019.

[15] S. Park, O. Bastani, N. Matni, and I. Lee, “Pac confidence sets for deep neural networks via calibrated prediction,” *arXiv preprint arXiv:2001.00106*, 2019.

[16] A. N. Angelopoulos, S. Bates, A. Fisch, L. Lei, and T. Schuster, “Conformal risk control,” *arXiv preprint arXiv:2208.02814*, 2022.

[17] R. Kaur, S. Jha, A. Roy, S. Park, E. Dobriban, O. Sokolsky, and I. Lee, “idecode: In-distribution equivariance for conformal out-of-distribution detection,” *Proceedings of the AAAI Conference on Artificial Intelligence*, vol. 36, no. 7, pp. 7104–7114, Jun. 2022. [Online]. Available: <https://ojs.aaai.org/index.php/AAAI/article/view/20670>

[18] R. Kaur, K. Sridhar, S. Park, S. Jha, A. Roy, O. Sokolsky, and I. Lee, “Codit: Conformal out-of-distribution detection in time-series data,” *arXiv preprint arXiv:2207.11769*, 2022.

[19] R. Luo, S. Zhao, J. Kuck, B. Ivanovic, S. Savarese, E. Schmerling, and M. Pavone, “Sample-efficient safety assurances using conformal prediction,” in *Algorithmic Foundations of Robotics XV: Proceedings of the Fifteenth Workshop on the Algorithmic Foundations of Robotics*. Springer, 2022, pp. 149–169.

[20] R. Tumu, L. Lindemann, T. Nghiem, and R. Mangharam, “Physics constrained motion prediction with uncertainty quantification,” *arXiv preprint arXiv:2302.01060*, 2023.

[21] D. Stutz, Krishnamurthy, Dvijotham, A. T. Cemgil, and A. Doucet, “Learning optimal conformal classifiers,” 2022.

[22] C. Xu and Y. Xie, “Conformal prediction for dynamic time-series,” *arXiv preprint arXiv:2010.09107*, 2020.

[23] I. Gibbs and E. Candès, “Conformal inference for online prediction with arbitrary distribution shifts,” *arXiv preprint arXiv:2208.08401*, 2022.

[24] A. Bhatnagar, H. Wang, C. Xiong, and Y. Bai, “Improved online conformal prediction via strongly adaptive online learning,” *arXiv preprint arXiv:2302.07869*, 2023.

[25] W. Wisniewski, D. Lindsay, and S. Lindsay, “Application of conformal prediction interval estimations to market makers’ net positions,” in *International Symposium on Conformal and Probabilistic Prediction with Applications*, 2020.

[26] A. Dixit, L. Lindemann, S. Wei, M. Cleaveland, G. J. Pappas, and J. W. Burdick, “Adaptive conformal prediction for motion planning among dynamic agents,” 2022. [Online]. Available: <https://arxiv.org/abs/2212.00278>

[27] K. M. Cohen, S. Park, O. Simeone, P. Popovski, and S. Shamai, “Guaranteed dynamic scheduling of ultra-reliable low-latency traffic via conformal prediction,” *arXiv preprint arXiv:2302.07675*, 2023.

[28] S. Hochreiter and J. Schmidhuber, “Long short-term memory,” *Neural computation*, vol. 9, no. 8, pp. 1735–1780, 1997.

[29] S. X. Wei, A. Dixit, S. Tomar, and J. W. Burdick, “Moving obstacle avoidance: A data-driven risk-aware approach,” *IEEE Control Systems Letters*, vol. 7, pp. 289–294, 2023.

[30] R. W. Cottle, J.-S. Pang, and R. E. Stone, *The linear complementarity problem*. SIAM, 2009.

[31] A. Bemporad and M. Morari, “Control of systems integrating logic, dynamics, and constraints,” *Automatica*, vol. 35, no. 3, pp. 407–427, 1999. [Online]. Available: <https://www.sciencedirect.com/science/article/pii/S0005109898001782>

[32] V. Raman, A. Donzé, M. Maasoumy, R. M. Murray, A. Sangiovanni-Vincentelli, and S. A. Seshia, “Model predictive control with signal temporal logic specifications,” in *53rd IEEE Conference on Decision and Control*. IEEE, 2014, pp. 81–87.

[33] R. Koenker and G. Bassett, “Regression quantiles,” *Econometrica*, vol. 46, no. 1, pp. 33–50, 1978. [Online]. Available: <http://www.jstor.org/stable/1913643>

[34] B. Yu, J. E. Mitchell, and J.-S. Pang, “Solving linear programs with complementarity constraints using branch-and-cut,” *Mathematical Programming Computation*, vol. 11, no. 2, pp. 267–310, 2019.

[35] S. Bradley, A. Hax, and T. Magnanti, *Applied Mathematical Programming*. Addison-Wesley Publishing Company, 1977. [Online]. Available: <https://books.google.com/books?id=MSWdWv3Gn5cC>

[36] Gurobi Optimization, LLC, “Gurobi Optimizer Reference Manual,” 2023. [Online]. Available: <https://www.gurobi.com>

[37] J. Van den Berg, M. Lin, and D. Manocha, “Reciprocal velocity obstacles for real-time multi-agent navigation,” in *2008 IEEE international conference on robotics and automation*. Ieee, 2008, pp. 1928–1935.

[38] P. Kothari, S. Kreiss, and A. Alahi, “Human trajectory forecasting in crowds: A deep learning perspective,” *IEEE Transactions on Intelligent Transportation Systems*, 2021.